

ION ENERGY AND ION ANGULAR DISTRIBUTIONS IN RF CAPACITIVELY COUPLED PLASMA SOURCES: PURE ARGON AND ARGON-OXYGEN MIXTURES

O.V. Manuilenko, K.M. Minaeva, V.I. Golota
NSC “Kharkov Institute of Physics and Technology”,
Academicheskaya Str. 1, 61108, Kharkov, Ukraine, e-mail:ovm@kipt.kharkov.ua

Single and dual frequency capacitively coupled plasma (CCP) sources operating in pure Ar, O₂ and Ar/O₂ mixtures are investigated by means of particle-in-cell/Monte Carlo collisions (PIC/MCC) simulations. The different possibilities to control ion energy distribution functions (IEDFs) and ion angular distribution functions (IADFs) on electrodes are found. It is shown that the driven voltage and frequency in single frequency capacitive discharges are control the IEDFs on the electrodes. It is demonstrated that the low frequency voltage in dual frequency CCP sources controls the IEDFs and IADFs. It is shown that the IEDFs on electrodes can be controlled by Ar/O₂ ratio.

PACS: 52.50.Dg, 52.80.Pi, 52.65.Rr, 52.65.Pp, 52.40.Kh, 52.77.Bn

1. INTRODUCTION

CCP sources [1] are widely used in the laboratory and in industry for a variety of processing techniques such as sputtering, deposition and etching. The interaction of energetic ions with solid surfaces plays a crucial role in these techniques. The positive ions accelerated through the space-charge sheath adjacent to the electrodes are responsible for the etch rates and depths, as well as for the etch profiles. Careful control of etch profiles is a basic requirement for a modern technologies. Etch profiles are defined by the IEDF and IADF on the wafer. In the present paper, the possibilities to control IEDFs and IADFs on electrodes in single and dual frequency CCP sources are investigated by means of PIC/MCC [2-6] simulations.

2. THE MODEL AND SIMULATION CONDITIONS

Weakly ionized plasmas in asymmetric single and dual frequency CCP sources have been studied in one dimension using the bounded electrostatic 1d3v PIC/MCC code [2-6]. The electron-neutral and ion-neutral collisions for pure Ar, pure O₂, and Ar/O₂ mixtures are included in the model via Monte Carlo [5]. The species modeled for Ar/O₂ mixtures are electrons, O₂⁺, O⁻, Ar⁺, excited argon atoms Ar*, excited oxygen molecules O₂* (rotational, vibrational, and electronic states), and background Ar and O₂. The full reaction set includes 33 reactions, but we trace just electrons, O₂⁺, Ar⁺, O⁻. The main channel for O⁻ formation is two-body dissociative attachment. The O₂⁻ are primarily formed in three-body reactions, the probability for which to occur is negligible for low-pressure discharges. Metastable Ar atoms are not considered. The resonant charge exchanges for O₂⁺ and Ar⁺, are included. The reactions between argon and oxygen include charge exchange between Ar and O₂⁺ and vice versa, scattering of positive and negative oxygen ions on Ar, scattering of Ar⁺ ions on O₂, and charge recombination.

The grid size Δx was small enough to resolve Debye length. The time step Δt was much less than the minimal time scale in the discharge. The “Courant condition for particles” was satisfied during modeling time. The modeling conditions are different for different runs, but the

scales are following: $\Delta t \in [10^{-12}, 10^{-11}]$ sec, $\Delta x \in [4 \cdot 10^{-4}, 4 \cdot 10^{-3}]$ cm. In conventional PIC/MCC simulations numerical fluctuations are inversely proportional to $\sqrt{N_{De} + N_{cell}}$, where N_{De} is the number of macroparticles per Debye length, and N_{cell} is the number of computer particles per cell. This numerical noise can increase the kinetic energy of the particles and creates substantial errors in the electron energy distribution function, electron temperature and plasma density. The influence of N_{cell} and N_{De} on the CCP source characteristics was studied in [6,7]. It was shown, that N_{cell} should be higher than 250 in the simulation. In each modeling case presented here from 250 to 1000 macro particles per cell was used.

3. RESULTS AND DISCUSSION

Figure 1 shows the IEDFs on the powered electrode for various driven voltages V_{hf} in the single frequency 30 MHz Ar discharge at 70 mTorr. As it is shown in Fig. 1, the IEDFs have fine structure, which is typical for low pressure discharges under following conditions: there are few charge-exchange collisions on the sheath length, and ion transit time through sheath τ_{ion} is greater than RF period τ_{hf} . These peaks are arisen because of acceleration of slow ions, which are created in the sheath as the result of charge-exchange collisions, by varying sheath potential. The number of peaks can be estimated as

$$N = \frac{\tau_{ion}}{\tau_{hf}} = \frac{1}{\pi \sqrt{2\eta}}, \quad (1)$$

where $\eta = eU / 4\pi^2 M f_{hf}^2 s^2$, $U = V_p - V_{dc}$ is the bias voltage, V_{dc} is the self-bias potential, V_p is the plasma potential, f_{hf} is the driven frequency, s is the sheath thickness, e is the ion charge, and M is the ion mass. As it follows from (1), and confirms by Fig. 1, the number of peaks decreases with increasing bias voltage U and, so with increasing driven voltage V_{hf} .

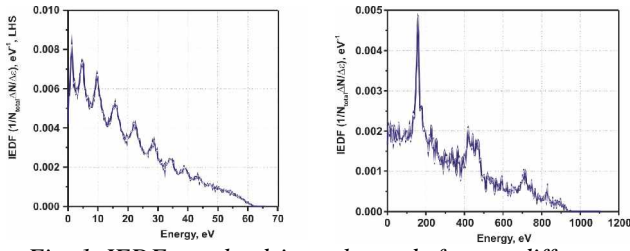


Fig. 1. IEDFs on the driven electrode for two different driven voltages V_{hf} (80 V for left graph, and 1300 V for right graph)

Figure 2 shows the IEDFs on the powered electrode for two driven frequencies. The peak structures are clearly visible. As follows from (1) and the scaling law for the sheath length [6] $s \propto f_{hf}^{-0.8}$, the number of peaks depends weakly on the frequency. The IEDF changes drastically as the driven frequency increases. With the increase frequency the relative number of high energy ions increases with a consequent decrease in the number of low energy ions. At high frequency (Fig. 2, right graph), when $s/\lambda_i \propto 3$, where λ_i is the ion mean free path, the IEDF exhibits a saddle-shaped structure. This structure is due to ions that passed through the sheath without collisions. It is centred around the dc sheath voltage U . At low frequencies (Fig. 2, left graph), when $s/\lambda_i \propto 10$, the bimodal structure disappears. The number of peaks obtained in the modelling is in good agreement with (1).

To control independently ion fluxes onto electrodes and ion energy, the dual frequency CCP source is used. The plasma density (ion flux) can be controlled by the high frequency RF power. The ion bombardment energy on the surface is defined by the low frequency (LF) power. The IEDFs on the powered electrode for two different LF voltages in the Ar dual frequency CCP source are presented in Fig. 3. The fine structure, observed in the single frequency case (Figs. 1,2), and in the case of small LF drive (Fig. 3, left graph), is destroyed as LF voltage increases (Fig. 3, right graph). This can be explained by the growth of the sheath length ($s \propto V_{lf}$, [6]) and, so, by increasing of the collisional parameter s/λ_i . For the left graph in Fig. 3, this parameter approximately 10, and for right IEDF in the Fig. 3, it is 20.

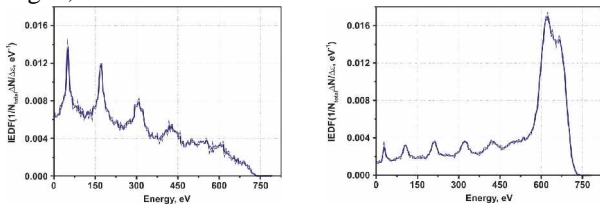


Fig. 2. IEDF on the driven electrode for two frequencies (30 MHz left graph and 130 MHz right graph) at driven voltage 1200 V and pressure 50 mTorr

Figure 4 shows the IADFs on the powered electrode for various LF voltages. As follows from figure 4, a large amount of ions strike the surface within an angle of about 3° . The IADF maximum is shifted with the LF voltage towards the low angles. The IADFs are widespread: a significant fraction of the ions impinge with highly off-normal angles.

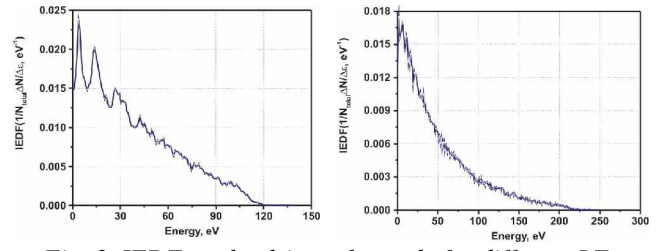


Fig. 3. IEDF on the driven electrode for different LF (2 MHz) voltages (20 V for left graph, and 250 V for right graph). Pressure 70 mTorr, high frequency voltage 160 V, frequency 30 MHz

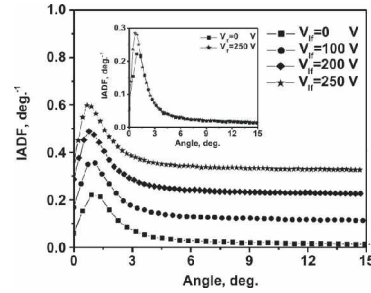


Fig. 4. IADFs on the powered electrode for different LF (2 MHz) voltages. High frequency (30 MHz) voltage is 160 V, pressure 70 mTorr. Vertical scales have been shifted to separate plots. Unshifted IADFs for two values of low frequency voltage are shown in the inset of the figure

Fig. 5 shows the IEDFs on the powered electrode for various Ar/O₂ ratios. The O₂⁺ IEDFs become more collisional with increase of relative oxygen density. The Ar⁺ IEDFs are less collisional for high oxygen case and more collisional for the mixtures with low oxygen concentration.

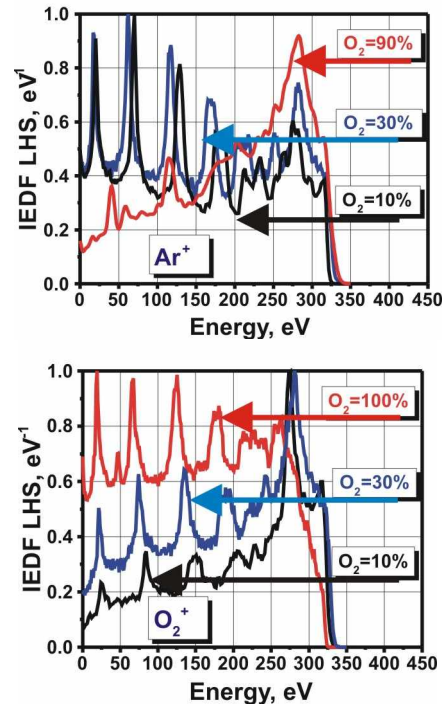


Fig. 5. IEDFs on the powered electrode for various Ar/O₂ ratios. Pressure = 35 mTorr, voltage 450 V, frequency 30 MHz

For small admixture of O_2 , when O_2^+ ions are not dominant, we observe typical collisionless distribution with abundance of high-energy ions. For a O_2 mixing ratio of 10%, sufficiently narrow bimodal energy distribution for O_2^+ ions is observed. This bimodal structure is due to the RF modulation of the ion energy as the O_2^+ ions pass the sheath. The situation changes with the increase of O_2 percentage. For 90% (or 100%) O_2 we obtain a typical collisional distribution with sufficiently high population of low-energy ions. The opposite trend is observed for the Ar^+ IEDF. When Ar^+ ions are dominant (10% O_2 in the mixture) the distribution is of collisional type. With 90% O_2 in the mixture Ar^+ ions do not dominate and the Ar^+ IEDF is collisionless. This IEDFs behaviour is determined by the charge exchange collisions. Ar^+ ions are effectively involved in symmetric resonant charge exchange processes with Ar neutrals, but not with O_2 neutrals. Thus, we have many resonant $Ar^+ + Ar$ collisions for a 10% O_2 mixing ratio when Ar^+ are dominant ions and few collisions for a 90% O_2 mixing ratio when Ar^+ ions are not the dominant species. This effect of transition from a collisionless to a collisional IEDF is analogous to the pressure increase effect outlined in [3]. However, in this case, instead of total pressure the partial pressure of certain gases must be considered.

In conclusion, the IEDF on the powered electrode in asymmetric single and double frequency capacitive discharges in Ar , O_2 and Ar/O_2 mixtures has been investigated with PIC/MCC simulations. It has been demonstrated that the IEDF shape and width can be controlled by the driven voltage in a single frequency CCP. It has been found that an increase in the driven frequency leads to significant changes in the IEDF shape, increasing the relative number of high energy ions and decreasing the number of low energy ions. The IEDF width does not change if the frequency increases. It has been demonstrated that the width of the IEDF is increased by growth

of the low frequency voltage in a double frequency CCP, and the fine structure observed in the single frequency case disappears simultaneously. It has been demonstrated that the low frequency voltage in dual frequency CCP sources controls the IADFs. It has been shown that the IEDFs on electrodes can be controlled by Ar/O_2 ratio.

REFERENCES

1. F.F.Chen. RF Plasma Sources for Semiconductor Processing. *Advanced Plasma Technology*. New York: "Wiley", 2006.
2. C.K. Birdsall and A.B.Langdon. *Plasma Physics via Computer Simulation*. New York: "Hilger", 1991.
3. J.K. Lee, N.Y. Babaeva, O.V. Manuilenko, H.C. Kim, J.W. Shon. Simulation of Capacitively Coupled Single and Dual frequency RF Discharges // *IEEE Transactions on Plasma Science*. 2004, v.32, N1, p.47-53.
4. J.K. Lee, O.V. Manuilenko, N.Y. Babaeva, H.C. Kim, J.W. Shon. Ion energy distribution control in single- and dualfrequency capacitive plasma sources // *Plasma Sources Science and Technology*. 2005, v. 14, N1, p. 89 - 97.
5. V. Vahedi, M. Surendra. Monte Carlo Collision Model for PIC Method: Application to Argon and Oxygen Discharges // *Comp. Phys. Commun.* 1996, v. 87, N2, p. 179 – 198.
6. O.V. Manuilenko, K.M. Minaeva. Ion Energy and Angular Distributions in RF Capacitively Coupled Plasma Sources. // *Problems of Atomic Science and Technology. Ser.: Plasma Electronics and New Methods of Acceleration*. 2006, N 5, p. 116 – 121.
7. H.C. Kim, F. Iza, S.S. Yang, M. Radmilović-Radjenić, J.K. Lee. Particle and fluid simulations of low-temperature plasma discharges: benchmarks and kinetic effects // *J. Phys. D: Appl. Phys.* 2005, v. 38, N9, R283–R301.

ФУНКЦИИ РАСПРЕДЕЛЕНИЯ ИОНОВ ПО ЭНЕРГИЯМ И УГЛАМ В ИСТОЧНИКАХ ПЛАЗМЫ НА ОСНОВЕ ВЫСОКОЧАСТОТНОГО ЕМКОСТНОГО РАЗРЯДА: ЧИСТЫЙ АРГОН И АРГОН-КИСЛОРОДНЫЕ СМЕСИ

О.В. Мануйленко, Е.М. Минаева, В.И. Голота

С помощью численного моделирования методом макрочастиц изучены одно- и двухчастотные источники плазмы на основе емкостного разряда (ЕР) в чистом Ar , O_2 и в Ar/O_2 смесях. Найдены способы управления функциями распределения ионов по энергиям (ФРИЭ) и углам (ФРИУ) на электродах. Показано, что ФРИЭ можно управлять с помощью амплитуды и частоты высокочастотной накачки, поддерживающей разряд в случае одночастотного ЕР. Показано также, что ФРИЭ и ФРИУ можно управлять с помощью величины амплитуды низкочастотного сигнала в источниках плазмы на основе двухчастотного ЕР. Показано, что ФРИЭ можно управлять с помощью изменения концентраций аргона/кислорода в Ar/O_2 смесях.

ФУНКЦІЇ РОЗПОДІЛУ ІОНІВ ЗА ЕНЕРГІЯМИ ТА КУТАМИ У ДЖЕРЕЛАХ ПЛАЗМИ НА ОСНОВІ ВИСОКОЧАСТОТНОГО ЄМКІСНОГО РОЗРЯДУ: ЧИСТИЙ АРГОН ТА АРГОН-КИСНЕВІ СУМІШІ

О.В. Мануйленко, К.М. Минаева, В.І. Голота

За допомогою числового моделювання методом макрочастинок досліджено одно- та двохчастотні джерела плазми на основі емкісного розряду (ЄР) у чистому Ar , O_2 , а також у Ar/O_2 сумішах. Знайдено способи керування функціями розподілу іонів за енергіями (ФРІЕ) та кутами (ФРІК) на електродах. Показано, що ФРІЕ можна керувати за допомогою амплітуди і частоти високочастотної накачки, що підтримує розряд у одно частотному джерелі плазми. Показано також, що ФРІЕ та ФРІК можна керувати за допомогою амплітуди низькочастотного сигналу у джерелі плазми на основі двох частотного ЄР. Показано, що ФРІЕ можна керувати за допомогою зміни концентрацій аргона/кисню у Ar/O_2 сумішах.